Polymer 50 (2009) 1281–1287

Contents lists available at ScienceDirect

Polymer

journal homepage: www.elsevier.com/locate/polymer

Local structure and composition of the ionic aggregates in Cu(II)-neutralized poly(styrene-*co*-methacrylic acid) ionomers depend on acid content and neutralization level

Wenqin Wang [a], Tsung-Ta Chan [a], Andrew J. Perkowski [b], Shulamith Schlick [b], Karen I. Winey [a,*]

[a] Department of Materials Science and Engineering, University of Pennsylvania, 3231 Walnut Street, Philadelphia, PA 19104-6272, United States
[b] Department of Chemistry and Biochemistry, University of Detroit Mercy, Detroit, MI 48221-3038, United States

ARTICLE INFO

Article history:
Received 27 October 2008
Received in revised form
22 December 2008
Accepted 4 January 2009
Available online 14 January 2009

Keywords:
Ionomers
Morphology
X-ray scattering

ABSTRACT

The morphologies of poly(styrene-*ran*-methacrylic acid) (SMAA) copolymers neutralized with Cu(II), including the local structure and composition of the ionic aggregates, were investigated as a function of acid content and level of neutralization. X-ray scattering and scanning transmission electron microscopy (STEM) results suggested that the sizes of the ionic aggregates in Cu(II)-neutralized SMAA are independent of the acid content and neutralization level. The number density of ionic aggregates increased slightly with acid content and neutralization level, but the increase was significantly less than expected for aggregates of fixed composition. Electron spin resonance (ESR) spectra of Cu(II) detected three distinct cation sites whose relative amounts changed with acid content. These results combined to indicate that the ionic aggregates contain non-ionic species and that the aggregate compositions become more ionic with increasing acid content and neutralization level.

© 2009 Elsevier Ltd. All rights reserved.

1. Introduction

Ionomers are copolymers containing a small fraction of ionic functional groups, which are often pendant to the polymer backbone [1]. Most of these ionic functional groups and their counterions self-assemble into ionic aggregates, due to the strong electrostatic interactions in the low dielectric constant media. These ionic aggregates act as physical cross-links that confer remarkable physical and chemical properties to the ionomers. Much research has been devoted to studying the sizes and spatial distribution of ionic aggregates using X-ray scattering [2–5], neutron scattering [6–8], and scanning transmission electron microscopy (STEM) [9–11]. The appearance of a broad, isotropic scattering peak at scattering vector $q = 1$–$5\ \mathrm{nm}^{-1}$ indicates the existence of ionic aggregates, and STEM enables direct imaging of the ion-rich aggregates. Winey's group has recently applied both STEM and X-ray scattering to investigate the size and number density of spherical ionic aggregates in a poly(styrene-*ran*-methacrylic acid) (SMAA) copolymer neutralized with Cu(II) [11,12]. By accounting for the extensive overlap in the STEM image, the images and the scattering data as interpreted by a liquid-like modified hard-sphere model are in excellent agreement with respect to both aggregate size (R_1) and aggregate number density (N_p). The successful reconciliation between STEM images and X-ray scattering for Cu(II)-neutralized SMAA ionomers demonstrates that the liquid-like modified hard-sphere model is able to reliably provide quantitative information about the size and number density of ionic aggregates in Cu(II)-neutralized SMAA ionomers. Having confidence in the scattering model allows us to explore the composition of the ionic aggregates [12].

The composition of the ionic aggregates is a critical part in any model of ion mobility or transport [13]. However, few studies have probed the composition of the ionic aggregates and it remains a subject of controversy whether ionic aggregates contain purely ionic groups or a mixture of ionic groups and non-ionic segments of the polymer chains [14]. The most widely used model, namely the "multiplet" model, presumes that the ionic aggregates contain only ionic groups [15,16]. Since the composition of ionic aggregates is strongly correlated with the local structure at the cations, most of the studies have been focused on the local environment and specific ligation of the ions in ionomers using Fourier transform infrared (FTIR) [17–19] and electron spin resonance (ESR) [20–22] spectroscopies. In an FTIR study of the local structures of poly(ethylene-*ran*-methacrylic acid) (EMAA) copolymer neutralized by Zn(II) with different neutralization levels, the acid groups were found to coexist in four distinct states: free acid, acid dimer, tetracoordinated zinc carboxylates, and hexacoordinated zinc carboxylates [17]. Early ESR studies of ionomers containing

* Corresponding author. Tel.: +1 215 898 0593; fax: +1 215 573 2128.
E-mail address: winey@seas.upenn.edu (K.I. Winey).

0032-3861/$ – see front matter © 2009 Elsevier Ltd. All rights reserved.
doi:10.1016/j.polymer.2009.01.007

carboxylic and sulfonic acids neutralized with transition metals (Mn(II) and Cu(II)) have detected both isolated cations and cation–cation dimers [23–25]. The study of Cu(II) in ionomeric systems by Schlick's group has shown that ESR spectra can provide a detailed picture of the type and number of ligands and of the strength of the interactions between the counterion and the ligand [26–30]. Kruczala and Schlick studied by ESR the interactions between ion-containing polymers and Cu(II) in aqueous media as a function of pH and temperature, and deduced the presence of two types of cation–acid complexes, corresponding to cation ligation to one and two carboxylic groups [31]. However, these spectroscopy studies fail to provide insight about the composition of the ionic aggregates.

The objective of this paper is a self-consistent description of the SMAA ionomer morphologies that correlates the local structure and composition in the ionic aggregates with the size and number density of the ionic aggregates. The ionic interactions between the methacrylic acid groups and the counterions were examined by ESR spectroscopy, while X-ray scattering and STEM probed the nanoscale ionic aggregates. This is the first time STEM, X-ray scattering and ESR have been combined in a single study, thereby overcoming the inconsistency in materials or preparation methods from separate studies. Furthermore, this paper extends our previous investigation of Cu-neutralized SMAA ionomers to include the influence of the acid content and the level of neutralization.

2. Experimental section

2.1. Materials and sample preparation

Poly(styrene-*ran*-methacrylic acid) (SMAA) copolymers with different mole fractions of acid were prepared by bulk free radical polymerization according to the procedures described elsewhere [32]. The copolymerization reaction time was controlled to achieve a conversion $\leq$10% in order to prevent heterogeneity in chemical structures in the later stage of the reaction. The acid contents of copolymers were measured by nuclear magnetic resonance (NMR). The weight average molecular weight of SMAA, as determined by gel permeation chromatography using a polystyrene standard, was $\sim 7 \times 10^5$ g/mol for copolymers with lower acid content (4.1 mol% and 5.8 mol%), and $\sim 4 \times 10^5$ g/mol for copolymers with higher acid content (7.2 mol%, 8.3 mol% and 13.3 mol%) with a polydispersity index of $\sim$2.0. SMAA copolymers were neutralized by first dissolving the copolymers in toluene. A stoichiometric amount of dehydrated copper(II) acetate was dissolved in methanol and added slowly into the gently agitated SMAA toluene solution to achieve 35%, 50%, or 100% of neutralization. The volume ratio of toluene to methanol was 9:1. The solution mixture was stirred overnight with gentle reflux at $\sim$100 °C. The Cu(II)-neutralized SMAA (SMAA–Cu) ionomers were recovered by solvent casting at room temperature for 1–2 days. Solvent casting was used, because previous results have shown that rapid precipitation produces non-equilibrium structures with inhomogeneous assemblies of ionic aggregates [33]. The materials were then dried under vacuum at 90 °C for 2 days and annealed under vacuum at 120 °C for 1 day to remove the acetic acid and residual solvent. All materials were stored at room temperature in vacuum desiccators. The acid content is given as the mole fraction x and the neutralization level as a percentage: SMAA$_x$–yCu. For example, SMAA$_{0.041}$–50Cu is a SMAA copolymer with 4.1 mol% acid and neutralized to 50% with Cu(II). It should be noted that our sample preparation method is reproducible, so the results are indicative of the material. The SMAA ionomers we prepared were studied by X-ray scattering, STEM, and ESR, to provide data that can be reliably integrated.

2.2. X-ray scattering

The solvent-cast, dried, and annealed ionomer films (0.1–0.5 mm thick) were used directly for X-ray scattering characterization. Our multi-angle X-ray scattering (MAXS) apparatus generates Cu X-ray from a Nonius FR 591 rotating-anode generator operated at 40 kV and 85 mA. The beam is focused by doubly-focusing mirror-monochromator optics in an integral vacuum system. The scattering data were collected over an interval of 1 h using a Bruker Hi-Star multiwire detector with a sample to detector distance of 11 cm. The 2-D analysis and model fitting were performed using *Datasqueeze* software [34].

The scattering data of SMAA–Cu ionomers were modeled with three functions:

$$I(q) = I_{KT}(q) + L_1(q) + L_2(q) \quad (1)$$

where $I_{KT}(q)$ is the Kinning–Thomas liquid-like hard-sphere model [35,36] used to interpret the ionomer peak, and $L_1(q)$ and $L_2(q)$ are Lorentzian functions used to fit the two polystyrene-related peaks, as previously reported [11]. The Kinning–Thomas model is the modified version of the Yarusso–Cooper model [5,35,36], where the Percus–Yevick [37] total correlation function that accounts for correlations between all particles in the system was used instead of the Fournet [38] three-body interference function.

2.3. Scanning transmission electron microscopy (STEM)

STEM specimens were sectioned from solvent-cast, dried, and annealed ionomer films at room temperature using a Reichert-Jung ultramicrotome with a diamond knife to a nominal thickness of 30–50 nm. STEM experiments were performed using a JEOL 2010F field emission transmission electron microscope. High-angle annular dark field (HAADF) images were recorded using a 0.7 nm STEM probe and a 70 μm condenser aperture at an accelerating voltage of 200 keV.

2.4. Electron spin resonance (ESR)

ESR spectra were recorded with a Bruker X-band EMX spectrometer operating at 9.7 GHz with 100 kHz magnetic field modulation, and equipped with the ER 4111 VT variable temperature unit and the Acquisit 32 Bit WINEPR data system version 3.01 for acquisition and manipulation. The microwave frequency was measured with a Hewlett–Packard 5350B microwave frequency counter. Typical instrumental parameters were as follows: sweep width 1000 G, microwave power 2 mW, time constant 5.12–20.48 ms, 10–16 scans depending on signal intensity, 2048 points per scan, and typical modulation amplitude 5 G.

3. Results and discussion

3.1. Room-temperature ionomer morphologies

HAADF STEM images of SMAA–Cu samples show spherical, uniformly distributed bright features, corresponding to Cu-rich ionic aggregates within a matrix of lower average atomic number. Fig. 1 depicts a representative STEM image for SMAA$_{0.133}$–50Cu. The intensity profiles taken across individual bright features were fit with Gaussian functions, and the diameters of the ionic aggregates were given by the full width at half maximum (FWHM) of the Gaussian functions [11]. The average diameters and their standard deviations for four SMAA–Cu ionomers are shown in Table 1. Taking into account the extensive projection overlap in the STEM images and the limit of instrumental resolution, STEM images indicate that

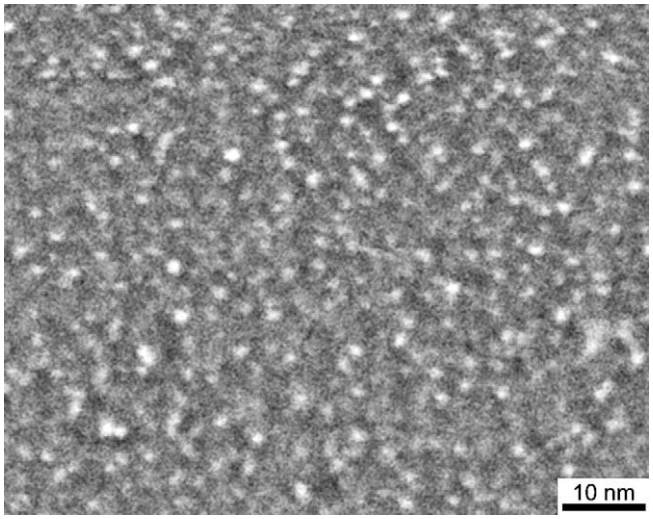

Fig. 1. HAADF STEM image of $SMAA_{0.133}$–50Cu shows a uniform distribution of spherical ionic aggregates.

the sizes of ionic aggregates are independent of the acid content and neutralization level.

The X-ray scattering profiles of SMAA–Cu ionomers show three isotropic peaks: polystyrene amorphous halo ($\sim$13 nm^{-1}), polymerization peak ($\sim$7 nm^{-1}), and ionomer peak (3–4 nm^{-1}), Fig. 2. A molecular dynamic simulation study of atactic polystyrenes by Ayyagari et al. [39] has found that the amorphous peak arises mainly from phenyl–phenyl correlation, and the polymerization peak is due primarily to intermolecular backbone–backbone correlations. While the two higher angle peaks are typical features in the scattering patterns of atactic polystyrenes and un-neutralized SMAA copolymers, the ionomer peak indicates the formation of nanoscale ionic aggregates. As the acid content increases, the relative intensity of the ionomer peak with respect to the polystyrene amorphous peak increases significantly at both 100% and 50% neutralization, Fig. 2a and b, respectively. The intensity of the ionomer peak also increases with neutralization level in $SMAA_{0.133}$–Cu, Fig. 3. The angular position of the ionomer peak is nearly independent of acid content and level of neutralization.

The ionomer peak of the SMAA–Cu ionomers was fitted with a liquid-like modified hard-sphere model based on four parameters: the radius of ionic aggregates R_1, the radius of closest approach R_{CA}, the number density of the aggregates N_p, and the amplitude A (note that $N_p = 1/V_p$, where V_p is the sample volume per ionic aggregate) [11]. X-ray data from $SMAA_{0.041}$ ionomers were not fitted due to the uncertainties inherent in a weak and broad ionomer peak in this material. In $SMAA_{0.133}$–100Cu, the strong ionomer peak obscures the polymerization peak ($\sim$7 nm) of polystyrene, thereby prohibiting a reliable fit. For all other ionomers, fits using Eq. (1) are shown in Figs. 2 and 3 and found to be in good agreement.

Table 1
Diameters of ionic aggregates obtained from STEM imaging and X-ray scattering.

Ionomer	D_{STEM} (nm)	$2R_{1,\ X\text{-}ray}$[a] (nm)
$SMAA_{0.072}$–100Cu	1.2 ± 0.3	1.16 ± 0.01
$SMAA_{0.083}$–100Cu	1.3 ± 0.4	1.15 ± 0.003
$SMAA_{0.133}$–100Cu	1.5 ± 0.3	N/A
$SMAA_{0.133}$–50Cu	1.2 ± 0.3	1.06 ± 0.008

[a] The standard deviations for $2R_{1,\ X\text{-}ray}$ are obtained when fitting the models to the X-ray scattering data. These values are only indicative of the numerical quality of the fits and not the uncertainties associated with the scattering model.

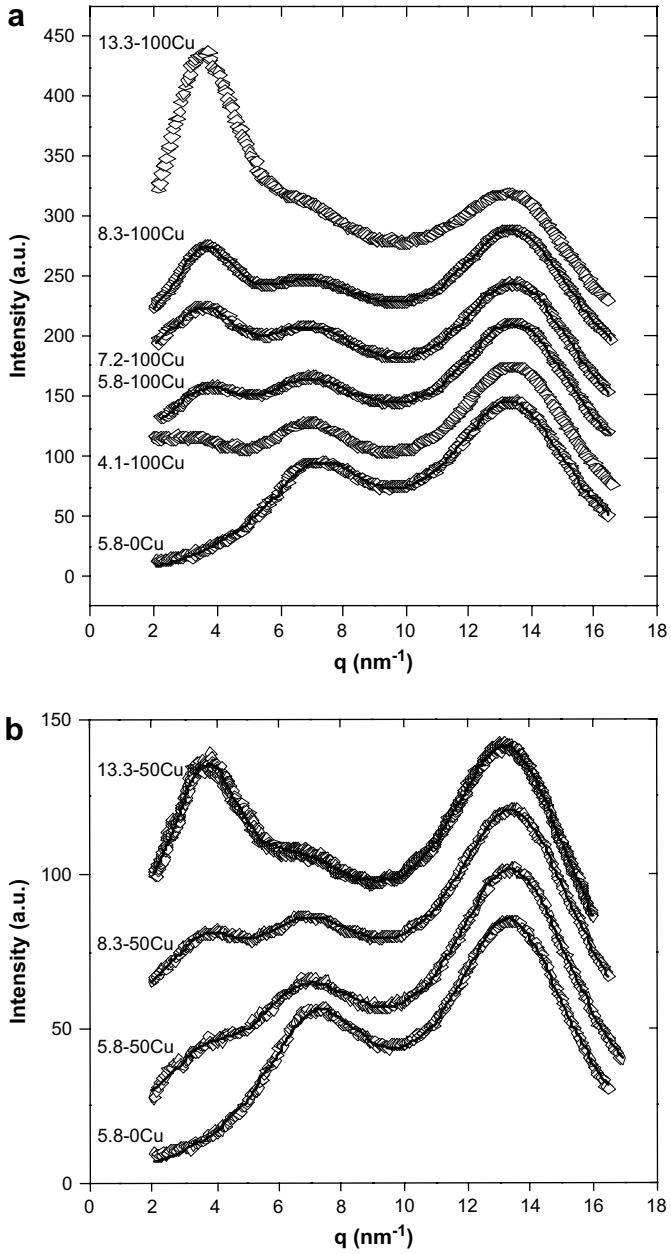

Fig. 2. X-ray scattering intensity (a.u.) as a function of scattering vector q with background scattering subtracted for different acid contents (4.1–13.3 mol%) neutralized with Cu(II) acetate along with the best-fit multi-function model given in Eq. (1) (solid line): a) 100% neutralization; b) 50% neutralization.

Selected samples have been probed by both STEM and X-ray scattering. Table 1 compares the size of the ionic aggregates (R_1) measured by these two methods and finds good agreement for this range of acid content. Furthermore, the STEM results verify that a liquid-like model of spherical ionic aggregates is appropriate for these SMAA–Cu ionomers prepared by solvent casting and annealing, as previously reported [11,12]. In contrast, recent work by the Winey group showed alternate morphologies for a $SMAA_{0.072}$–100Cu ionomer prepared by the precipitation method [33].

The R_1 and R_{CA} values for all the SMAA–Cu ionomers are shown in Fig. 4a. Neither the acid content (5.8–13 mol%) nor the level of neutralization (35–100%) significantly changes the ionic aggregate size (R_1) or the radius of closest approach (R_{CA}). These results in solvent-cast ionomers are consistent with several different

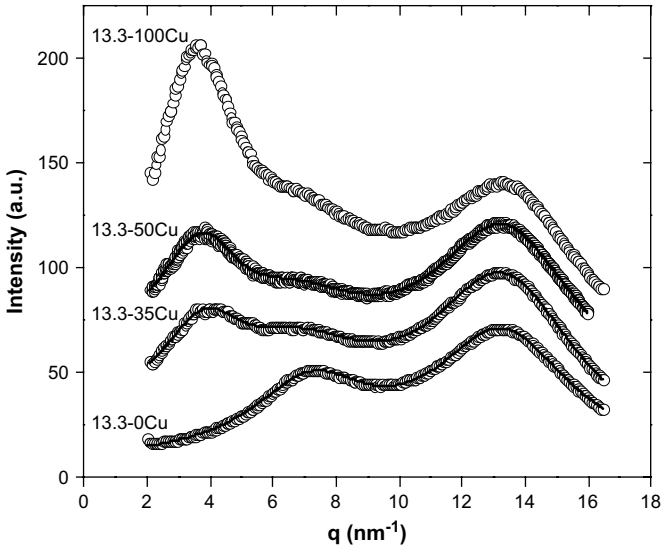

Fig. 3. X-ray scattering intensity (a.u.) as a function of scattering vector q with background scattering subtracted for $SMAA_{0.133}$ neutralized with Cu(II) acetate to different levels (0–100%) along with the best-fit multi-function model given in Eq. (1) (solid line).

ionomer systems studied by other groups [5,40]. Yarusso and Cooper have applied a similar liquid-like model to interpret the X-ray scattering profiles of sulfonated polystyrenes neutralized with zinc (SPS–Zn), and they also found that the sizes of ionic aggregate were independent of ion content (1.68–6.91 mol% acid, 20–90% neutralization) [5]. Tsujita et al. [40] found by X-ray scattering that when neutralized with divalent and trivalent cations, the radii of ionic aggregates in EMAA ionomers were hardly changed (3.5 and 5.4 mol% acid, 40–85% neutralization).

The X-ray scattering model also provides the number density of the aggregates (N_p), which increases only slightly with increasing acid content and neutralization level, Fig. 4b. In fact, the number of aggregates per volume increases to a much smaller extent than expected by assuming, as does the multiplet model, a constant ionic aggregate composition consisting of purely $Cu^2(COO^-)_2$. For example, if the acid content doubles at 100% neutralization, the multiplet model predicts that the number density of ionic aggregation should double. Similarly, if the level of neutralization increases from 50% to 100% at a fixed acid content, N_p should also double. However, the difference in the measured N_p is much less than predicted by the multiplet model when the neutralization level increases from 50% (filled triangles) to 100% (filled squares): 12% increase at 5.8 mol% and 19% increase at 8.3 mol%. Fig. 4 suggests that the ionic aggregates incorporate non-ionic species. In contrary to the multiplet model, if all the un-neutralized COOH groups are incorporated into the ionic aggregates of SMAA–Cu ionomers, N_p is expected to increase by a factor of only 1.3 as the neutralization level increases from 50% to 100%. This ratio is closer to our experimental data, supporting our conclusion that ionic aggregates contain COOH groups in partially neutralized ionomers. When the neutralization level increases, the new ionic groups are predominately incorporated into the existing ionic aggregates and thereby form few new aggregates.

In these SMAA–Cu ionomers, R_1 is nominally constant and N_p increases by <20% as the level of neutralization increases from 50% to 100%. These observations cast doubt on the assumptions of the widely used multiplet model of ionic aggregates in our partially neutralized SMAA–Cu ionomers, namely that the ionic aggregates contain only ionic species. Using rheological data and FTIR spectroscopy, Vanhoorne and Register have also found that acid groups

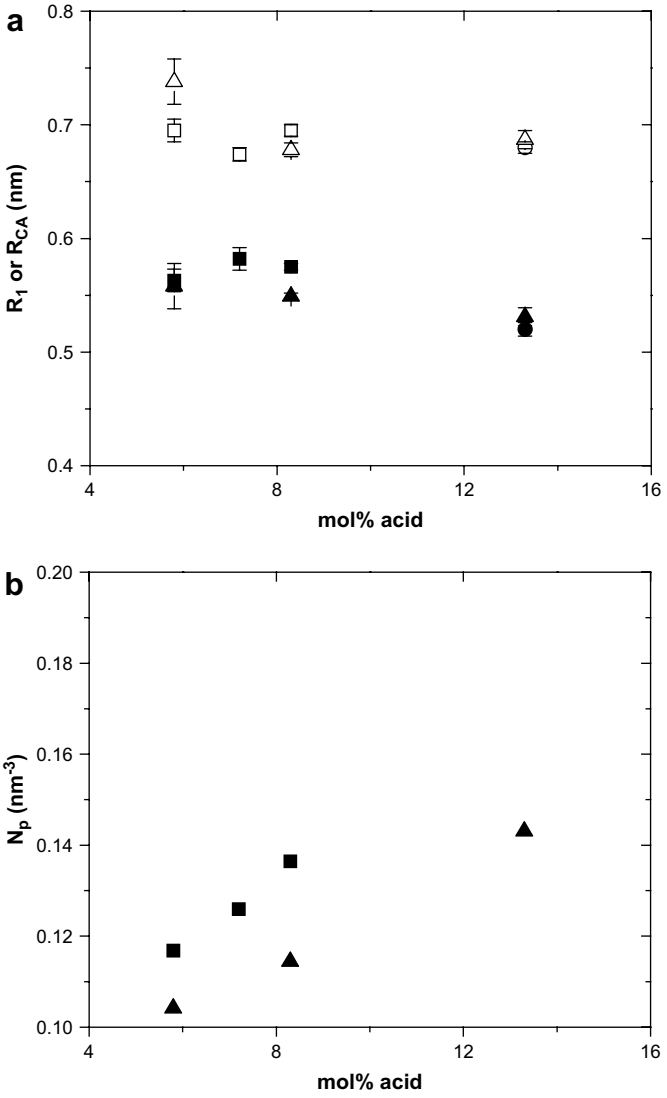

Fig. 4. a) R_1 (filled) and R_{CA} (open) determined by X-ray scattering as a function of acid content for different levels of neutralization with Cu(II) acetate: □,■ 100%; △,▲ 50%; ○,● 35%. The error bar represents the error of the fitting parameter generated by a least-square fit. b) The number density of the ionic aggregate (N_p) as a function of acid content from X-ray scattering results: ■ 100% neutralization; ▲ 50% neutralization.

are associated with the ionic aggregates in poly(ethylene-methacrylic acid) ionomers (EMAA) partially neutralized with Na [13]. However, when EMAA ionomers are neutralized with Zn, a transition metal, their data suggested that the COOH groups are in the matrix rather than the ionic aggregates [13]. Specifically, COOH groups form reversible dimers with each other through hydrogen bonding in the un-neutralized and certain partially neutralized EMAA and SMAA ionomers [13,41,42]. Our results for SMAA ionomers partially neutralized with Cu might suggest that the COOH could both form dimers and reside in the ionic aggregates. Thus, the following question arises from our SMAA–Cu ionomer systems: are the excess acid groups for partially neutralized SMAA–Cu ionomers distributed in the polymer matrix or in the ionic aggregates, and how does the acid content affect the distribution? If the acid groups are preferentially associated with the aggregates, how does it affect the coordination structures of cations in the ionic aggregates? To address these questions, ESR spectroscopy experiments were performed on these same ionomers to probe the local structure around the counterions.

3.2. Local ionomer morphology

Fig. 5 presents the temperature variation of the ESR spectra for $SMAA_{0.083}$–50Cu. In general terms, these ESR spectra for Cu(II) in SMAA are similar to those previously detected for Cu(II) in poly(ethylene-*co*-methacrylic acid) (EMAA) ionomers [31]. In both systems the spectra indicate complete immobilization of the cation even at ambient temperature (293 K in SMAA and 300 K in EMAA), due to ligation to oxygen atoms from the carboxylic groups. Moreover, the resolution is improved at lower temperatures, because of longer Cu(II) spin–lattice relaxation time. The perpendicular component, represented by the quartet in the range 3200–3300 G is difficult to interpret due to the presence of forbidden transitions. For this reason, conclusions are based on the parallel region, which is characterized by large $g_{\|}$- and hyperfine splitting ($A_{\|}$) values of the Cu nucleus ($I = 3/2$). The parallel spectrum is typical of the "strain" effect, arising from a distribution of the g and hyperfine splitting that lead to different widths of each signal, depending on the nuclear spin magnetic quantum number m_I. The spectra at 110 K allow the identification of two sites, site 1 and site 2 in Fig. 5, based on different values of the $g_{\|}$ and $A_{\|}$: site 1, $A_{\|} = 129$ G (142×10^{-4} cm^{-1}), $g_{\|} = 2.355$; site 2, $A_{\|} = 153$ G (165×10^{-4} cm^{-1}), $g_{\|} = 2.308$ (Table 2). Although the presence of two cation sites is clear from the spectra given in Fig. 5, more accurate and complete parameters for both sites would require ^{63}Cu enrichment and spectra simulations.

The spin-forbidden transition from binuclear Cu–Cu complexes is expected at a magnetic field of ≈1600 G, and the distance between the two cations in the dimer can be deduced from the intensity ratio of signals from the mononuclear and dimeric complexes, as documented in the case of Nafion perfluorinated ionomers neutralized by Cu(II) [43]. Signals from the dimeric species were not detected in the SMAA–Cu ionomers, suggesting that the mononuclear Cu(II) complexes are well separated by the polymer chains.

Fig. 6a presents the ESR spectra at 110 K of SMAA–50Cu samples containing 5.8, 8.3 and 13.3 mol% acid. Qualitatively, the spectra indicate that site 2 is the major site in all three partially neutralized ionomers. There is evidence for a third site for $SMAA_{0.058}$–50Cu, with $A_{\|} = 167$ G (177×10^{-4} cm^{-1}), and $g_{\|} = 2.275$. Another ESR spectrum of $SMAA_{0.058}$–50Cu is shown in Fig. 6b, for an ionomer sample that was hot pressed at 145 °C for 10 min after annealing. The spectra from the two preparations are very similar, but the resolution in the pressed sample is improved, allowing the clearer identification of site 3. At 50% neutralization, increasing the acid

Table 2
Magnetic parameters for the Cu(II) complexes detected by ESR in the STEM ionomers.[a]

	$g_{\|}$	$A_{\|}$/G	$A_{\|}/10^4$ cm^{-1}
Site 1	2.355	129	142
Site 2	2.308	153	165
Site 3	2.275	167	177

[a] $A_{\|}$ (cm^{-1}) $= g_{\|} \times A_{\|}$(G) $\times 4.667 \times 10^{-5}$.

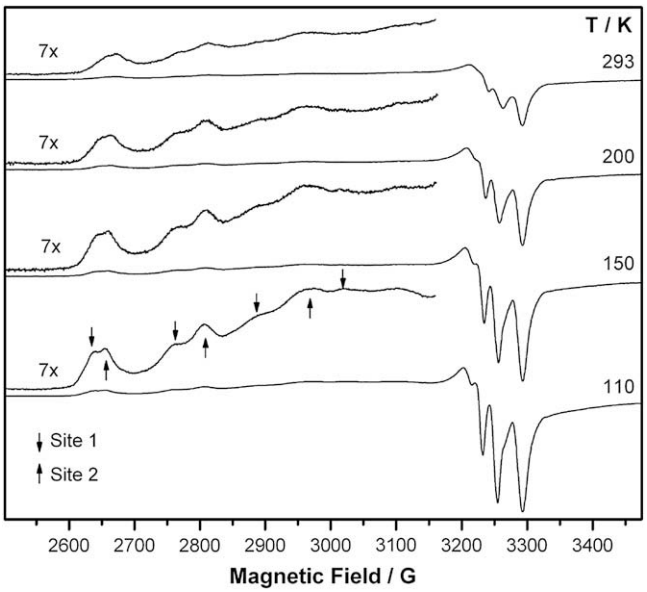

Fig. 5. X-band ESR spectra of $SMAA_{0.083}$–50Cu as a function of temperature. Vertically expanded portions are shown for all spectra. Downward and upward arrows indicate, respectively, the parallel hyperfine quartet for site 1 and site 2.

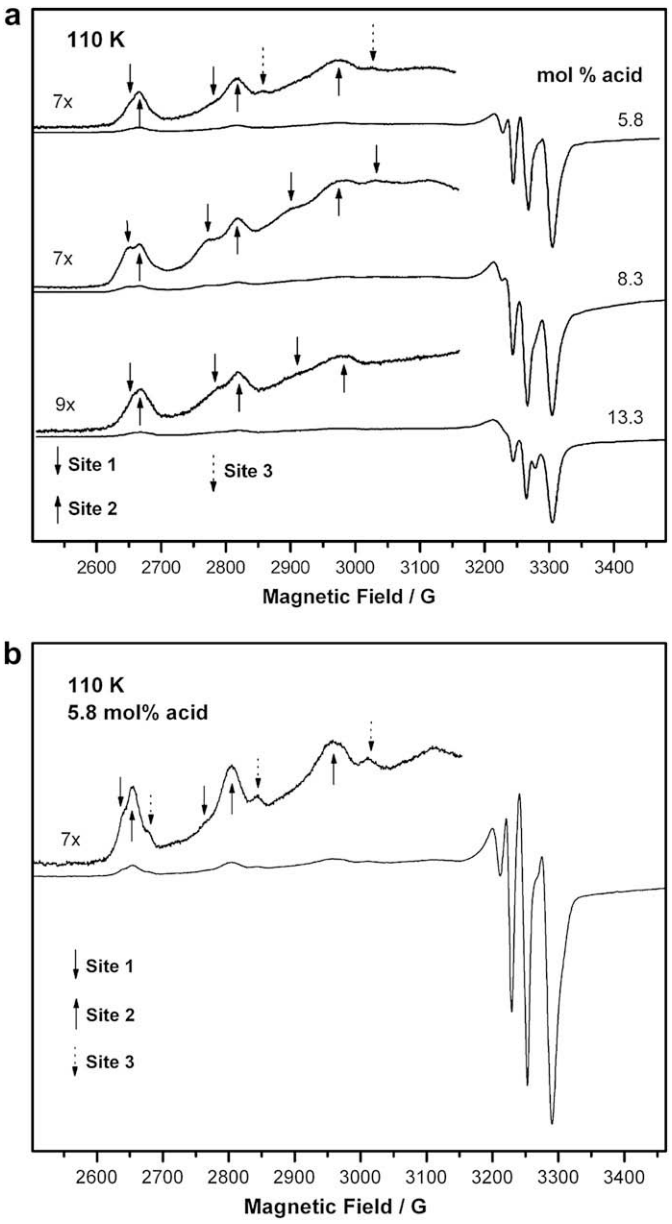

Fig. 6. a) X-band ESR spectra at 110 K of SMAA–50Cu containing 5.8, 8.3, and 13.3 mol% acid. b) X-band ESR spectra at 110 K of $SMAA_{0.058}$–50Cu after hot pressing. Vertically expanded portions are shown for all spectra. Note: the arrows (downward, upward, and dotted) indicate the positions of the parallel hyperfine signals for sites 1–3, and the improved resolution in the spectrum of the hot-pressed sample.

content apparently reduces the number of sites to two. The change in the relative population of the three different cation sites clearly shows the variation of local environment around copper cations with acid content. The magnetic parameters for sites 1–3 above are listed in Table 2.

The $g_{\|}$ and $A_{\|}$ values in Cu(II) complexes are sensitive to the binding scheme, as described in detail in the Peisach–Blumberg (PB) plots [44]. All ligands in the Cu(II) complexes in the SMAA ionomers are oxygens. If the oxygen ligands originate from charged groups such as COO^- groups, these plots predict a decrease in the $g_{\|}$ value and an increase in the $A_{\|}$ value compared to the magnetic parameters of the $Cu(H_2O)_6^{2+}$ complex, where all ligands are neutral and $g_{\|} > 2.4$ and $A_{\|} = 120$ G ($\sim 134 \times 10^{-4}$ cm^{-1}) [31]. These expectations are clearly seen in the parameters for sites 1–3 in Table 2; qualitatively, these parameters reflect an increase in the number of oxygen ligands from charged groups, in this case COO^- groups, from site 1 to site 2 and to site 3. In addition, the PB plots suggest for sites 1–3 complexes with total charges in the vicinity of +1, 0, and −1 respectively. In the case of site 1 this deduction implies two oxygen ligands from the negatively charged –COO^- and two additional oxygen ligands from undissociated acid groups –COOH. For site 2 and a total charge of 0, the ESR parameters indicate Cu(II) complexation with four oxygen ligands from two –COO^- groups. Similarly, the number of oxygen ligands for site 3 suggests a Cu(II) complex with three COO^- groups. These deductions are semiquantitative and final values of the g values and Cu hyperfine splitting should be determined by ^{63}Cu enrichment and simulation of the spectra.

All ESR spectra of the fully neutralized SMAA ionomer, SMAA–100Cu, consist of rather broad lines and show a site with $A_{\|} = 155$ G, very close to the major site (site 2) in SMAA–50Cu; see Supporting information. The spectra of fully neutralized SMAA–Cu ionomers also suggest the formation of more ordered structures at 13.3 mol% compared to SMAA–100Cu with lower acid contents. Due to the limited resolution, it is impossible to determine the type of sites in the fully neutralized ionomers. Nevertheless, the qualitative results are in agreement with the scattering and imaging results, which indicate that upon increasing the neutralization level fewer new ionic aggregates are formed, but the ionic aggregates incorporate more acid–cation pairs.

The ESR conclusions are in contrast to X-ray absorption studies in EMAA ionomers: Grady et al. [45] found identical local environments around zinc atoms in all zinc-neutralized EMAAs for different preparation methods, acid contents and neutralization levels. However, the work of Farrell and Grady on sodium-neutralized EMAA ionomers detected disordered local environments around the cation that are highly dependent on neutralization levels [46], as also seen in our ESR results. The contrast in our ESR results for SMAA–Cu ionomers and the X-ray absorption results for EMAA–Zn ionomers could simply reflect the differences in copolymer type, cation, neutralization method, or thermal processing. Alternatively, the distinct results could be associated with differences in sensitivity for the two methods. Given that ESR is only applicable when ionomers are neutralized with paramagnetic cations, such as copper, an interesting next step would be to use X-ray absorption to study Cu-neutralized ionomers in conjunction with the powerful combination of STEM, X-ray scattering and ESR.

Based on the fact that the number density of the ionic aggregates (N_p) increases by <20% slightly when the percent of neutralization doubles (Fig. 4b), we conclude that a considerable fraction of un-neutralized acid groups are incorporated into the ionic aggregates when ionomers are partially neutralized. This is consistent with the presence of multiple local environments in partially neutralized SMAA–Cu via ESR (Fig. 6) as well as with the absence of Cu–Cu dimers mentioned above. ESR results also show that the relative intensity of different sites varies with acid content, thus reflecting the sensitivity of the method to the structure and composition of the ionic aggregates in ionomers.

4. Conclusions

The morphologies, compositions, and coordination structures of ionic aggregates in a wide range of Cu(II)-neutralized SMAA ionomers have been studied by a combination of X-ray scattering, HAADF STEM imaging, and ESR spectroscopy. The sizes of the spherical ionic aggregates are independent of acid content and neutralization level, as shown by both X-ray scattering and STEM. The composition of ionic aggregates is found to change with acid content and neutralization level based on the following two observations. 1) As the acid content or neutralization level doubles, the number density of ionic aggregates increases by a much smaller extent, which contradicts the widely-held assumption of constant aggregate composition. 2) ESR spectra show the presence of multiple disordered cation–acid coordination structures and the order of the local cation environment increases with acid content. Consequently, the ionic aggregates apparently contain non-ionic species, including un-neutralized acid groups, and the ionic aggregates incorporate fewer non-ionic species as the acid content increases. The strength of ionic association and ion mobility are strongly related to the local structure and composition of these ionic aggregates. Our findings provide valuable information for other ionomers with carboxylic acids and for the understanding of ion diffusion and polymer dynamics in these ionomers. This systematic study using three complimentary methods can be extended to other acid types and paramagnetic cations for a broader investigation of the structure–property relationships in ion-containing polymers.

Acknowledgement

This work was supported by the National Science Foundation Polymers Program under Grant DMR 05-49116 (Winey) and DMR 0412582 (Schlick). The authors gratefully acknowledge the use of the vacuum line and GPC in Prof. Shu Yang's laboratory at the University of Pennsylvania. We also thank S.I. White and M.D. McConnell for their expertise during the SMAA copolymer synthesis and M.V. Motyakin for preliminary ESR experiments.

Appendix. Supporting information

ESR spectra of SMAA–100Cu ionomers with different acid contents. This material is available free of charge via the Internet at http://pubs.acs.org. Supplementary data associated with this article can be found in the online version, at doi:10.1016/j.polymer.2009.01.007.

References

[1] Eisenberg A, Kim JS. Introduction to ionomers. New York: John Wiley & Sons; 1998.
[2] MacKnight WJ, Taggart WP, Stein RS. J Polym Sci Polym Symp 1974;45(1):113–28.
[3] Marx CL, Caulfield DL, Cooper SL. Macromolecules 1973;6(3):344–53.
[4] Roche EJ, Stein RS, Russell TP, MacKnight WJ. J Polym Sci Part B Polym Phys 1980;18(7):1497–512.
[5] Yarusso D, Cooper SL. Macromolecules 1983;16(12):1871–80.
[6] Earnest TRJ, Higgins JS, Handlin DL, MacKnight WJ. Macromolecules 1981;14(1):192–6.
[7] Earnest TRJ, Higgins JS, MacKnight WJ. Macromolecules 1982;15(5):1390–5.
[8] Aldebert P, Dreyfus B, Pineri M. Macromolecules 1986;19(10):2651–3.
[9] Laurer JH, Winey KI. Macromolecules 1998;31(25):9106–8.
[10] Winey KI, Laurer JH, Kirkmeyer BP. Macromolecules 2000;33(2):507–13.
[11] Benetatos NM, Heiney PA, Winey KI. Macromolecules 2006;39(16):5174–6.

[12] Benetatos NM, Chan CD, Winey KI. Macromolecules 2007;40(4):1081–8.
[13] Vanhoorne P, Register RA. Macromolecules 1996;29(2):598–604.
[14] Grady BP. Polym Eng Sci 2008;48(6):1029–51.
[15] Eisenberg A. Macromolecules 1970;3(2):147–54.
[16] Eisenberg A, Hird B, Moore RB. Macromolecules 1990;23(18):4098–107.
[17] Coleman MM, Lee JY, Painter PC. Macromolecules 1990;23(8):2339–45.
[18] Brozoski BA, Coleman MM, Painter PC. Macromolecules 1984;17(2):230–4.
[19] Walters RM, Sohn KE, Winey KI, Composto RJ. J Polym Sci Part B Polym Phys 2002;40(24):2833–41.
[20] Kutsumizu S, Schlick S. J Mol Struct 2005;739(1–3):191–8.
[21] Kutzumizu S, Goto M, Yano S, Schlick S. Macromolecules 2002;35(16): 6298–305.
[22] Tsagaropoulos G, Kim JS, Eisenberg A. Macromolecules 1996;29(6):2222–8.
[23] Yamauchi J, Yano S. Makromol Chem 1988;189(4):939–50.
[24] Yamauchi J, Yano S. Macromolecules 1982;15(1):210.
[25] Weiss RA, Lefelar JA, Toriumi H. J Polym Sci Polym Lett Ed 1983;21(8):661–7.
[26] Szajdzinska-Pietek E, Schlick S. In: Schlick S, editor. Ionomers: characterization, theory, and applications. Boca Raton, FL: CRC Press; 1996 [chapter 7].
[27] Bednarek J, Schlick S. J Am Chem Soc 1990;112(13):5019–24.
[28] Bednarek J, Schlick S. J Am Chem Soc 1991;113(9):3303–9.
[29] Bednarek J, Schlick S. Langmuir 1992;8(1):249–53.
[30] Schlick S, Alonso-Amigo MG, Bednarek J. Colloids Surf A 1993;72:1–9.
[31] Kruczala K, Schlick S. J Phys Chem B 1999;103(11):1934–43 and references therein.
[32] Eisenberg A, Navratil M. Macromolecules 1973;6(4):604–12.
[33] Benetatos NM, Winey KI. Macromolecules 2007;40(9):3223–8.
[34] Heiney PA. Comm Powder Diffr Newsletter 2005;32:9–11.
[35] Kinning DJ, Thomas EL. Macromolecules 1984;17(9):1712–8.
[36] Zhou NC, Chan CD, Winey KI. Macromolecules 2008;41(16):6134–40.
[37] Percus JK, Yevick GJ. Phys Rev 1958;110(1):1–13.
[38] Fournet G. Acta Crystallogr 1951;4:293–301.
[39] Ayyagari C, Bedrov D, Smith G. Macromolecules 2000;33(16):6194–9.
[40] Tsujita Y, Yasuda M, Kinoshita T, Takizawa A, Yoshimizu H. Macromolecules 2001;34(7):2220–4.
[41] Earnest TR, Macknight WJ. J Polym Sci Part B Polym Phys 1978;16(1): 143–57.
[42] Arai K, Eisenberg A. J Macromol Sci Phys 1980;B17(4):803–32.
[43] Schlick S, Alonso-Amigo MG, Eaton SS. J Phys Chem 1989;93(23):7906–12.
[44] Peisach J, Blumberg WE. Arch Biochem Biophys 1974;162(2):502–12.
[45] Grady BP, Floyd JA, Genetti WB, Vanhoorne P, Register RA. Polymer 1999;40(2):283–8.
[46] Farrell KV, Grady BP. Macromolecules 2001;34(20):7108–12.